SUPPLEMENTARY APPENDIX

Blockade of crizotinib-induced BCL2 elevation in ALK-positive anaplastic large cell lymphoma triggers autophagy associated with cell death

Avedis Torossian,[1,2,3] Nicolas Broin,[1,2,3] Julie Frentzel,[1,2,3] Camille Daugrois,[1,2,3,4] Sarah Gandarillas,[5] Talal Al Saati,[6] Laurence Lamant,[1,2,3,4,7,8] Pierre Brousset,[1,2,3,4,7,8] Sylvie Giuriato,[1,2,3,8,9] and Estelle Espinos[1,2,3,4,8]

[1]Inserm, UMR1037 CRCT, F-31000 Toulouse, France; [2]Université Toulouse III-Paul Sabatier, UMR1037 CRCT, F-31000 Toulouse, France; [3]CNRS, ERL5294 UMR1037 CRCT, F-31000, Toulouse, France; [4]Laboratoire d'Excellence Toulouse-Cancer-TOUCAN, F-31024 Toulouse, France; [5]Inserm/UPS, US006/CREFRE, F-31000 Toulouse, France; [6]Inserm/UPS, US006/CREFRE, Service d'Histopathologie, F-31000 Toulouse, France; [7]Département de Pathologie, IUCT, F-31000 Toulouse, France; [8]European Research Initiative on ALK-related Malignancies (ERIA), Cambridge, UK and [9]Transautophagy: European network for multidisciplinary research and translation of autophagy knowledge, COST Action CA15138, Brussel, Belgium

 doi:10.3324/haematol.2017.181966

Received: October 11, 2017.

Accepted: January 22, 2019.

Pre-published: January 24, 2019.

Correspondence: *ESTELLE ESPINOS* - estelle.espinos@inserm.fr

SYLVIE GIURIATO - sylvie.giuriato@inserm.fr

Blockade of crizotinib-induced BCL2 elevation in ALK-positive anaplastic large cell lymphoma triggers autophagy associated with cell death

Avedis Torossian[1,2,3], Nicolas Broin[1,2,3], Julie Frentzel[1,2,3], Camille Daugrois[1,2,3], Sarah Gandarillas[4], Talal Al Saati[5], Laurence Lamant[1,2,3,6,7], Pierre Brousset[1,2,3,6,7], Sylvie Giuriato[1,2,3,7,8,] and Estelle Espinos[1,2,3,7]

[1]-INSERM, UMR1037 CRCT, Toulouse, France

[2]-Université Toulouse III-Paul Sabatier, UMR1037 CRCT, Toulouse, France

[3]-CNRS, ERL5294 UMR1037 CRCT, Toulouse, France

[4]- INSERM/UPS, US006/CREFRE, Toulouse, France

[5]- INSERM/UPS, US006/CREFRE, Service d'Histopathologie, Toulouse, France

[6]-Département de pathologie, IUCT, Toulouse, France

[7]-European Research Initiative on ALK-related malignancies (ERIA)

[8]-Transautophagy: European network for multidisciplinary research and translation of autophagy knowledge, COST Action CA15138

Supplemental Data

Supplemental Methods

miRNA and siRNA transfections

Transfections were performed by electroporation using Gene Pulser Xcell Electroporation Systems (Bio-Rad, Hercules, CA, USA). Briefly 5.10^6 cells were electroporated at 950 µF and 250 V in 400 µl serum-free IMDM medium with 100 nM siRNA or miRNA-mimics from a 100 µM stock solution or with the same quantity of negative controls (siCTL was purchased from Eurogentec and miR-Neg/4464058 was purchased from Ambion, ThermoFisher). The siRNA sequences used were 5'-GGGCGAGCUACUAUAGAAATT–3' for ALK, 5'-GCUGCACCUGACGCCCUUCTT-3' for BCL2, 5'- CGAGAUGAAUGUGAAUAUGAATT for MET and the siGENOME ULK1 siRNA (D-005049-01-0005, Dharmacon) for ULK1. The miRNA mimic used was mirVana miRNA mimic hsa-miR-34a-5p (MC22030) for miR-34a (Ambion, ThermoFisher). Following shock, cells were rapidly re-suspended in 5ml IMDM supplemented with 15% FCS, before being used for protein extraction, flow cytometry and viability/proliferation assays.

Protein extraction and western blot analysis

Cells were incubated for 10min on ice in RIPA-buffer (20mM Tris HCl pH 7.4, 150mM NaCl, 4mM EDTA, 0.5% Triton X-100, and 0.2% SDS) supplemented with protease and phosphatase inhibitors (2mM Na_3VO_4, 20mM NaF and 1mM PMSF, purchased from Sigma-Aldrich; complete protease inhibitor cocktail tables were purchased from Roche Applied Science). The cells were then subjected to 2 pulses of sonication (10 s each separated by a 30 s incubation on ice) using a Bioblock Vibra-cell 72446 apparatus at 40% of its power (Bioblock, San Diego, CA, USA). Insoluble material was eliminated by centrifugation (10min at 10 000 g, 4°C). The total protein concentration of cell lysates was determined using a Bradford assay. Protein lysates (30µg) were then fractionated by SDS-PAGE (10%), and transferred to a nitrocellulose membrane (Whatman) (GE Healthcare, Little Chalfont, England). Western-blotting was performed using antibodies against BCL2 (Santa-Cruz, C2, sc-7382), ALK (D5F3 XP, Cell Signaling Technology #3633), P-ALK (Y1604, Cell Signaling Technology, cs3341), β-actin (Santa Cruz #7210), LC3B (Nanotools, Teningen, Germany, #0231–100, 5F10, mouse mAb) , p62/ SQSMT1 (mAb,610832, BD Bioscience) , MET (Cell Signaling Technology, #8198) and ULK1 (Cell Signaling Technology, R600, #4773). Proteins were visualized using the Chemiluminescent Peroxidase Substrate-3 Kit (Sigma-Aldrich, France) or the ECL™ Clarity (Bio-Rad).

Cell cycle analysis using propidium iodide incorporation and flow cytometry

150 000 cells (per condition) were washed twice with PBS and fixed overnight at -20°C in 70% ethanol. Cells were then washed twice with PBS (0.1% BSA) and once with PBS only, before a 30min incubation with 30µg/ml propidium iodide (Invitrogen, ThermoFisher) and 500µg/ml RNAse A (Sigma-Aldrich). Thereafter, cells were analyzed on a MACSQuant VYB flow cytometer (Miltenyi Biotec, Santa Barbara, USA) and results were obtained using the FlowJo software (Dean Jett Fox model).

Caspase assay:

The Caspase-Glo 3/7 assay from Promega (Madison, WI, USA) was used to monitor cell apoptosis through measuring caspase activation, according to the manufacturer's instructions.

Generation of KARPAS-299 cells expressing a tandem fluorescent-tagged LC3 reporter protein (mRFP-EGFP-LC3)

As reported by Kimura et al.[1], the use of the mRFP-EGFP tandem fluorescent-tagged LC3 reporter protein for autophagy flux quantification takes advantage of the higher sensitivity of EGFP fluorescence to the acidic environment of the autolysosome relative to that of RFP. Autophagosomes labeled by this reporter protein exhibit both RFP and EGFP signals (yellow puncta in confocal analysis). However, after fusion with lysosomes, the EGFP signals of the newly-formed autolysosomes are attenuated whereas the RFP signals remain, producing red puncta, as revealed by confocal analysis. Thus, cells with higher flux are less green due to the fusion of autophagosomes with lysosomes and, accordingly, they display an increased RFP/EGFP ratio, as measured and quantified by flow cytometry[2].

To generate stable mRFP-EGFP-LC3-expressing KARPAS-299 cells (clonal cell population), $5x10^6$ exponentially growing cells were transfected with 5 µg of mRFP-EGFP-LC3 plasmid (kindly provided by Prof Tamotsu Yoshimori, Ozaka, Japan) by electroporation at 250 V and 950 µF using the Gene Pulser II Electroporation System (BioRad, Hercules, California). Stable transformants were selected in complete medium containing increasing concentrations of G418 (Sigma Aldrich), from 0.5mg/mL to 1.2mg/mL. For higher sensitivity and consistency, single cell sorting for RFP and EGFP double-positive cells was performed to isolate individual clones. One selected clone, called mRFP-EGFP-LC3 KARPAS-299, was further validated for autophagy flux activation upon crizotinib treatment, as previously reported by classical LC3 turnover assay performed on a whole population of KARPAS-299 ALK-positive ALCL cells[3]. This validation was done both by flow cytometry and by confocal imaging. In keeping with our former data that reported an accumulation of the LC3-II form following a kinetics of crizotinib treatment (see Figure 2E in Mitou et al. [3]), we observed an increase in the number of mRFP-EGFP-LC3 KARPAS-299 cells that exhibited high RFP/EGFP fluorescence ratios over time (Figure S6A). These data were obtained on a BD LSR Fortessa™ flow cytometer and the results were analyzed using the FlowJo software.

Moreover, we also noticed, using confocal imaging, that both yellow (autophagosome) and red (autolysosome) puncta were present in untreated cells that exhibited basal autophagy (Figure S6B, left panel) whereas most puncta were red in cells that exhibited crizotinib-induced autophagic flux (Figure S6B, right panel and Figure S6C for quantification).

Cyto-ID^{R}- based procedure for autophagy detection

The CYTO-ID^{R} autophagy detection kit (ENZ-51031-K200, Enzo Life Sciences, Inc) was used to detect autophagy vacuoles and monitor autophagy flux. Cells were seeded at 3 x 10^5 cells/mL and incubated for the indicated time with either rapamycin (100nM), Crizotinib (125nM to 500nM) or both drugs, in the presence or absence of chloroquine (CQ, 10µM), a known autophagy inhibitor, to allow the accumulation of autophagy vacuoles. The Cyto-ID® Green autophagy dye and the cell stainings were performed according to the manufacturer's instructions. The fluorescence of the cell samples (1x 10^5 cells/condition) was detected using a MACSQuant VYB (Miltenyi Biotec, Santa Barbara, USA) and the flow cytometry data were analyzed with the FlowJo software. As we did with the mRFP-EGFP-LC3 KARPAS-299 expressing cells, cyto-ID-stained cells were split into two groups: cells with low/basal autophagy flux and cells with high/induced autophagy flux, based on their relative intensity in the green fluorescence channel (FL1, 530nm).

Murine xenograft model

Mice were housed under specific pathogen-free conditions in an animal room at a constant temperature (20–22°C), with a 12 h/12 h light/dark cycle and free access to food and water. All animal procedures were performed following the principle guidelines of INSERM, and our protocol was approved by the Midi-Pyrénées Ethics Committee on Animal Experimentation.

A total of 4.10^6 KARPAS-299 cells were injected subcutaneously into both flanks of 6-week old female non-obese diabetic-severe combined immunodeficient (NOD-SCID) mice (Janvier Labs, Laval, France). Mouse body weight and tumor volumes were measured every day with calipers, using the formula "length × width^2 × π/6". Mice were treated 5 times per week (Monday through Friday) once the tumor volume reached 100mm^3, by receiving crizotinib (2.5mg/kg) or H_2O orally. At the end of the experiment, mice were humanely sacrificed. Subcutaneous tumors and adjacent inguinal lymph nodes were harvested and sections were fixed in 10% neutral buffered formalin for immunohistochemistry (IHC) analysis.

Immunohistochemistry

Sections from formalin-fixed and paraffin-embedded xenografted tumors were stained with hematoxylin and eosin. IHC analysis was performed using antibodies directed against LC3B (mouse mAb, 0231-100/LC3-5F10, dilution 1/100, Nanotools) and p62/SQSTM1 (mouse mAb,

#610833, dilution 1/100, BD, Biosciences). Antibody binding was detected with the streptavidin-biotin-peroxidase complex method (Vector Laboratories, Burlingame, CA, USA). Pictures were taken using either a Leica DM4000B microscope (Wetzlar, Germany) or a Panoramic 250 device (3DHISTECH, Budapest, Hungary).

Quantification of LC3B and p62 staining

LC3B positive dots from IHC staining as depicted in Figure 6 were quantified using the quantification module of the pannoramic viewer software (3D HISTECH); the quantification was performed on a total of 10 distinct areas of 0.012 and 0.044mm^2 (that include approximately 100 cells to 400 cells) on each tumor sections (Figure S12A). For the quantification of p62 staining, the evaluation of p62 dot-like staining was hindered in some case by strong cytoplasmic staining. For that reason, we could not use the automated quantification module of the pannoramic viewer software. Instead and as described by Schläfli et al. [4], we divided the dot-like staining patterns into an intensity score from 0 to 3 for quantitative evaluation as follows: score 0, no dots or barely visible dots in <5% of the cells; score 1, detectable dots in 5-25% of the cells; score 2, readily detectable dots in 25-75% of the cells; score 3, dots in >75% of the cells. The classification was performed on a total of 10 distinct areas of 0.012 (that include approximately 100 cells) on each tumor sections and by three different people (SGiu, NB and EE) (Figure S12B). Statistical analysis was performed by unpaired Student's t tests.

REFERENCES

1. Kimura S, Noda T, Yoshimori T. Dissection of the autophagosome maturation process by a novel reporter protein, tandem fluorescent-tagged LC3. Autophagy;3(5):452-460
2. Gump JM, Thorburn A. Sorting cells for basal and induced autophagic flux by quantitative ratiometric flow cytometry. Autophagy 2014;10(7):1327–1334.
3. Mitou G, Frentzel J, Desquesnes A, Le Gonidec S, AlSaati T, Beau I, et al. Targeting autophagy enhances the anti-tumoral action of crizotinib in ALK-positive anaplastic large cell lymphoma. Oncotarget;6(30):30149-30164.
4. Schläfli AM, Berezowska S, Adams O, Langer R, Tschan MP. Reliable LC3 and p62 autophagy marker detection in formalin fixed paraffin embedded human tissue by immunohistochemistry. Eur J Histochem 2015;59(2): 2481. doi10.4081/ejh.2015.2481.

FIGURE S1

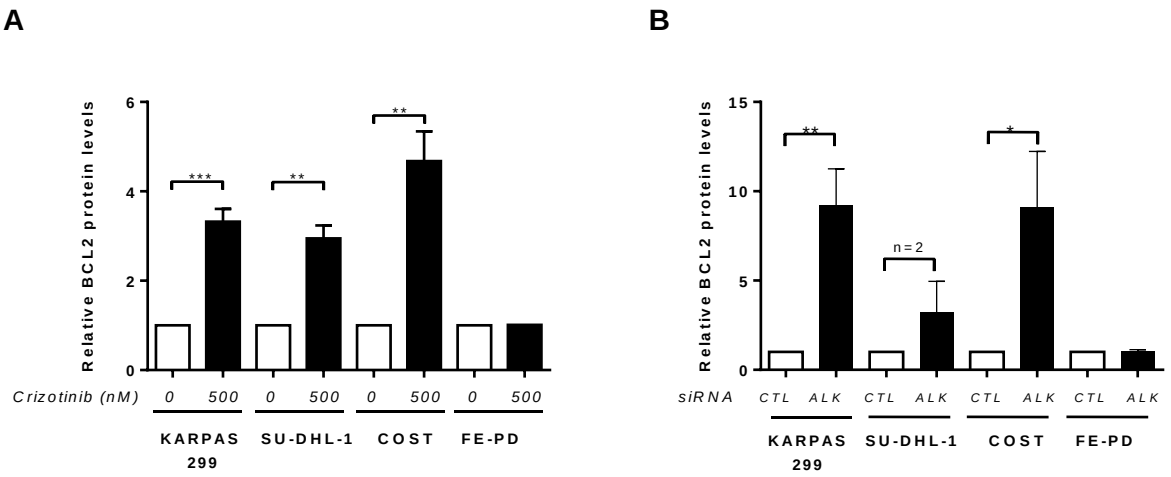

FIGURE S1. Quantification of increased BCL2 protein levels in response to NPM-ALK inactivation or following NPM-ALK downregulation. (A) Histogram representation of BCL2 protein levels in ALK-positive or ALK-negative ALCL cells that have been treated with crizotinib (500nM) for 24h. (B) Histogram representation of BCL2 protein levels in ALK-positive or ALK-negative ALCL cells transfected with either a negative control siRNA (siCTL) or a siRNA targeting ALK mRNA (siALK) for 72h. BCL2/β-actin signal ratios were quantified using GelQuantNET; this ratio was set to 1 for the untreated condition for each cell line. Data represent mean ± SEM; n=3 (n=2 for SU-DHL-1 cells); *p≤0.05; **p≤0.01; ***p≤0.001, unpaired Student's t test.

FIGURE S2

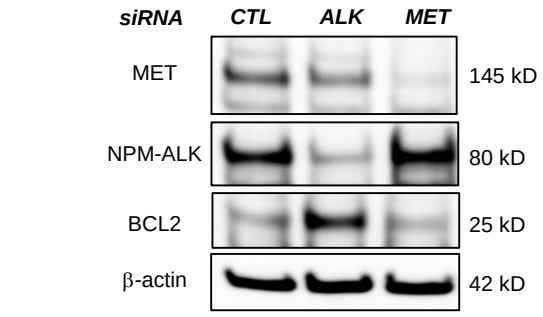

MET / β-actin	1	0,5	0,03
NPM-ALK / β-actin	1	0,1	1
BCL2 / β-actin	1	4,4	0,7

FIGURE S2. BCL2 protein levels are not modulated by MET downregulation.
Western blot analysis of MET, NPM-ALK and BCL2 protein levels in KARPAS-299 cells that were transfected with either a negative control siRNA (siCTL) or a siRNA targeting ALK (siALK) or MET (siMET) mRNAs for 72h. β-actin served as the internal control. Signal ratios were quantified using GelQuantNET and were set to 1 for the untreated condition. The data shown are representative of two independent experiments which gave similar results.

FIGURE S3

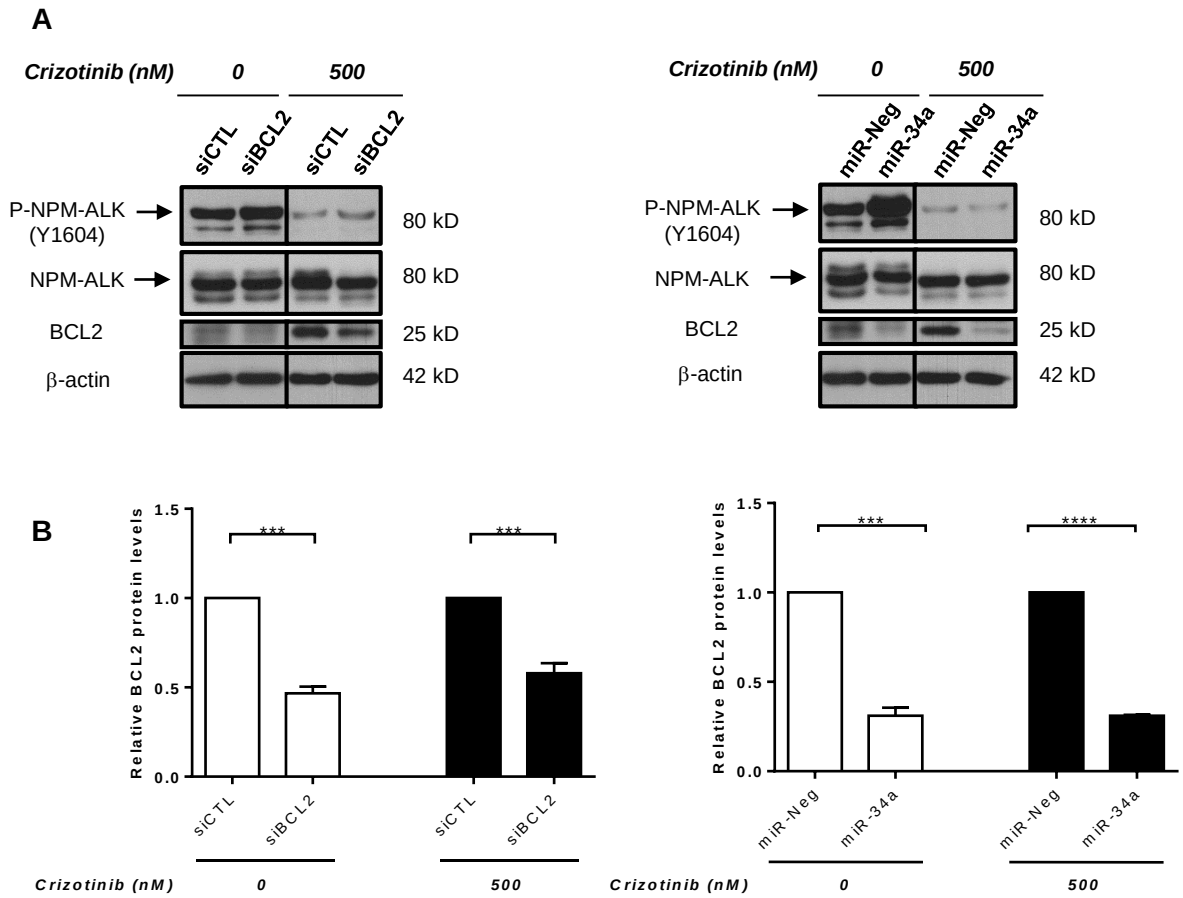

FIGURE S3. Silencing efficiencies of siBCL2 and miR-34a mimics. (A) Western blot analysis of BCL2 protein levels following BCL2 knockdown. Twenty-four hours after the transfection of a siBCL2 (left panel), miR-34a mimics (right panel), or their corresponding negative controls (siCTL or miR-Neg), ALK-positive ALCL cells were treated (or not) with crizotinib (500 nM) for 72h and BCL2 protein levels were assessed by western blotting. β-actin served as the internal control to ensure equal loading. (B) Histogram representations of BCL2 protein levels following BCL2 knockdown using either siBCL2 siRNA (left panel) or miR-34a mimics (right panel). BCL2 and β-actin signal were quantified using GelQuantNET; BCL2/β-actin was set to 1 for siCTL or miR-Neg condition. Data represent mean ± SEM. n=3; ***p≤0.001; ****p≤0.0001; unpaired Student's t test.

FIGURE S4

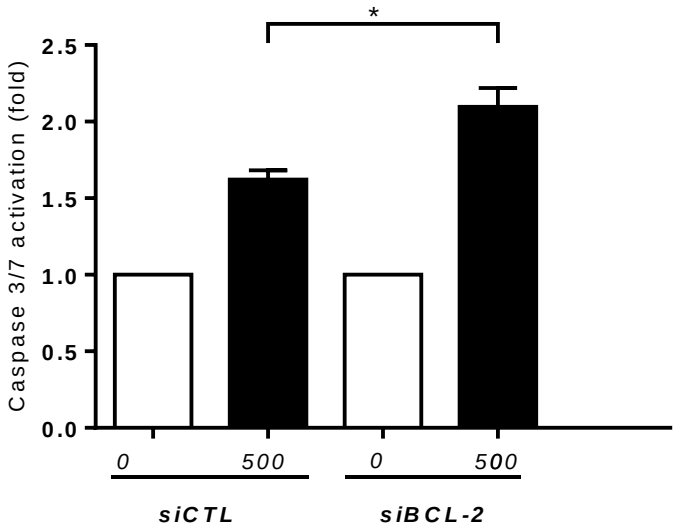

FIGURE S4. BCL2 downregulation using a targeted siRNA potentiates crizotinib-induced apoptotic cell death in KARPAS-299 cells. Twenty-four hours after the transfection of a targeted siRNA (siBCL2) or its negative control (siCTL), KARPAS-299 cells were treated (or not) with crizotinib (500nM) for 72h. Measurement of caspase 3/7 activation by caspase-Glo3/7 assay kit. Data represent mean ± SEM. n=3; *p ≤ 0.05; unpaired Student's t test.

FIGURE S5

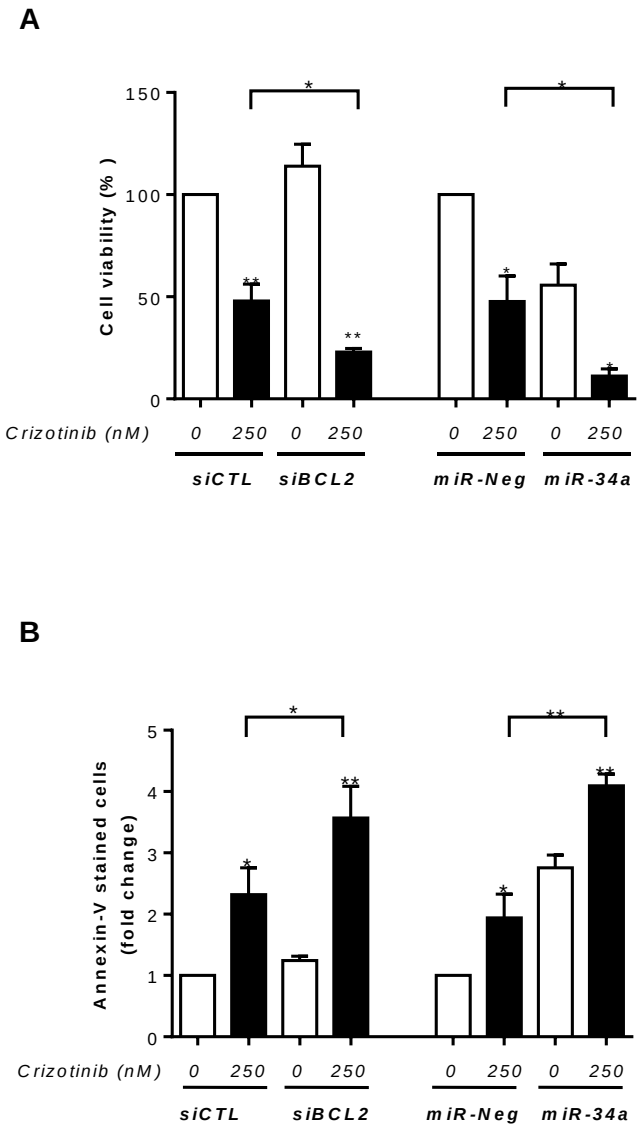

FIGURE S5. BCL2 downregulation potentiates crizotinib-induced loss in cell viability and apoptotic cell death in SU-DHL-1 cells. Twenty-four hours after the transfection of the BCL2-targeting interfering RNAs siBCL2 or miR-34a mimics, or their corresponding negative controls (siCTL or miR-Neg), SU-DH-L1 were treated (or not) with crizotinib (250nM) for 72h. (A) Cell viability was assessed by MTS colorimetric measurements. Data represent mean ± SEM. n=3; *p ≤ 0.05; **p ≤ 0.01; unpaired Student's t test. (B) Flow cytometry analysis of annexin V-positive SU-DHL-1 cells following the knockdown of BCL2 and crizotinib treatment. Graph represents fold change of Annexin V-stained cells from 3 independent experiments ± SEM. *p ≤ 0.05; **p≤0.01; unpaired Student's t test.

FIGURE S6

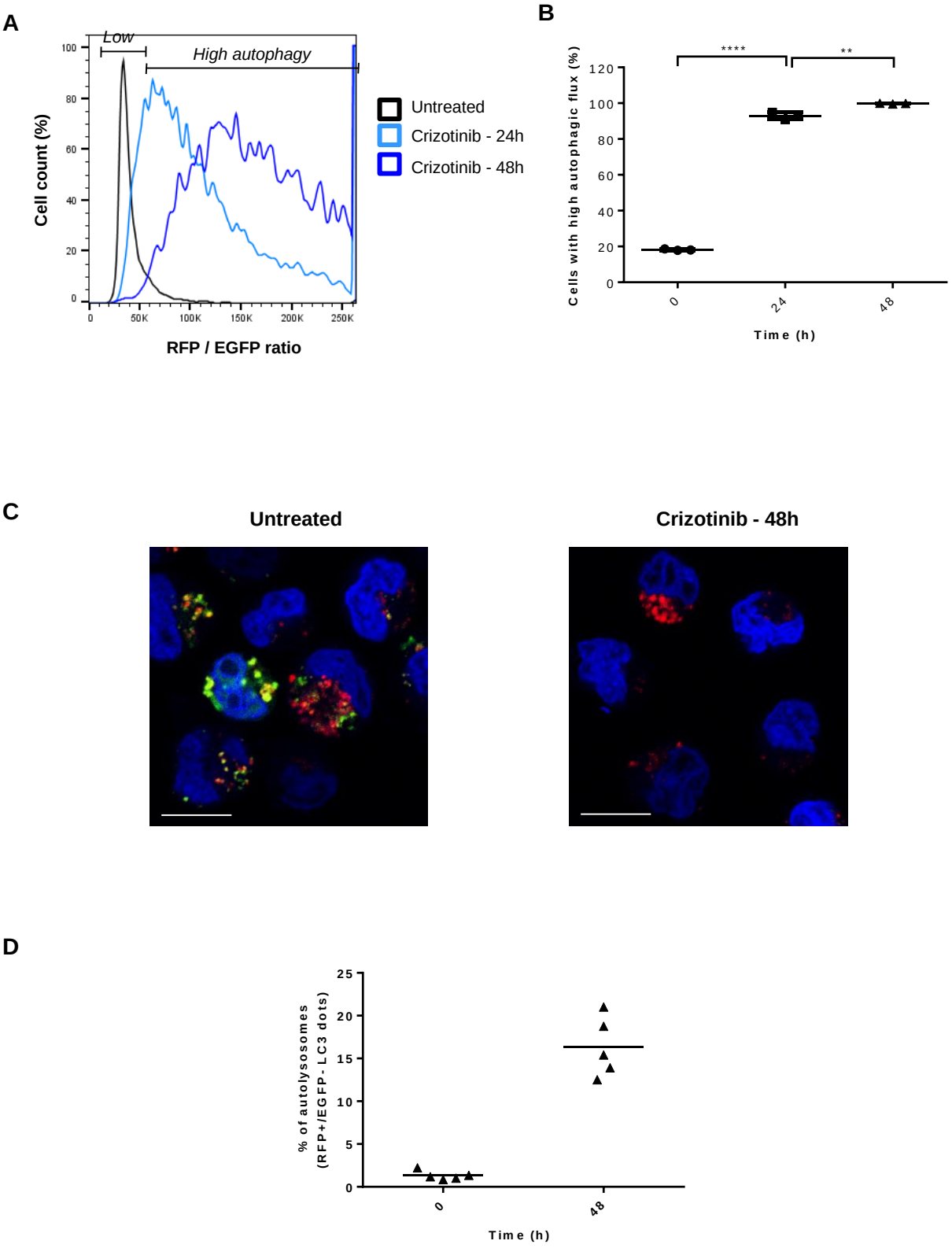

FIGURE S6. Validation of the use of tandem fluorescent-tagged LC3 reporter cells for autophagic flux monitoring. (A) Representative FACS plots showing the RFP/EGFP fluorescence ratios using flow cytometry in mRFP-EGFP-LC3 KARPAS-299 cells that have been treated with crizotinib (500 nM) for 0, 24 and 48 hours. (B) Histogram representation of enhanced autophagic flux in response to crizotinib treatment. Data represent mean ± SEM; n=3; **p≤0.01 ; ****p≤0.0001; unpaired Student's t test. (C) Confocal microscopy analysis of the above-mentioned cells. In green/red merged images, yellow puncta (i.e, RFP+, EGFP+) indicate autophagosomes, while red puncta (i.e, RFP+, EGFP-) indicate autolysosomes. Scale bars represent 10µm. (D) Histogram representation of the quantification of autolysosomes.

FIGURE S7

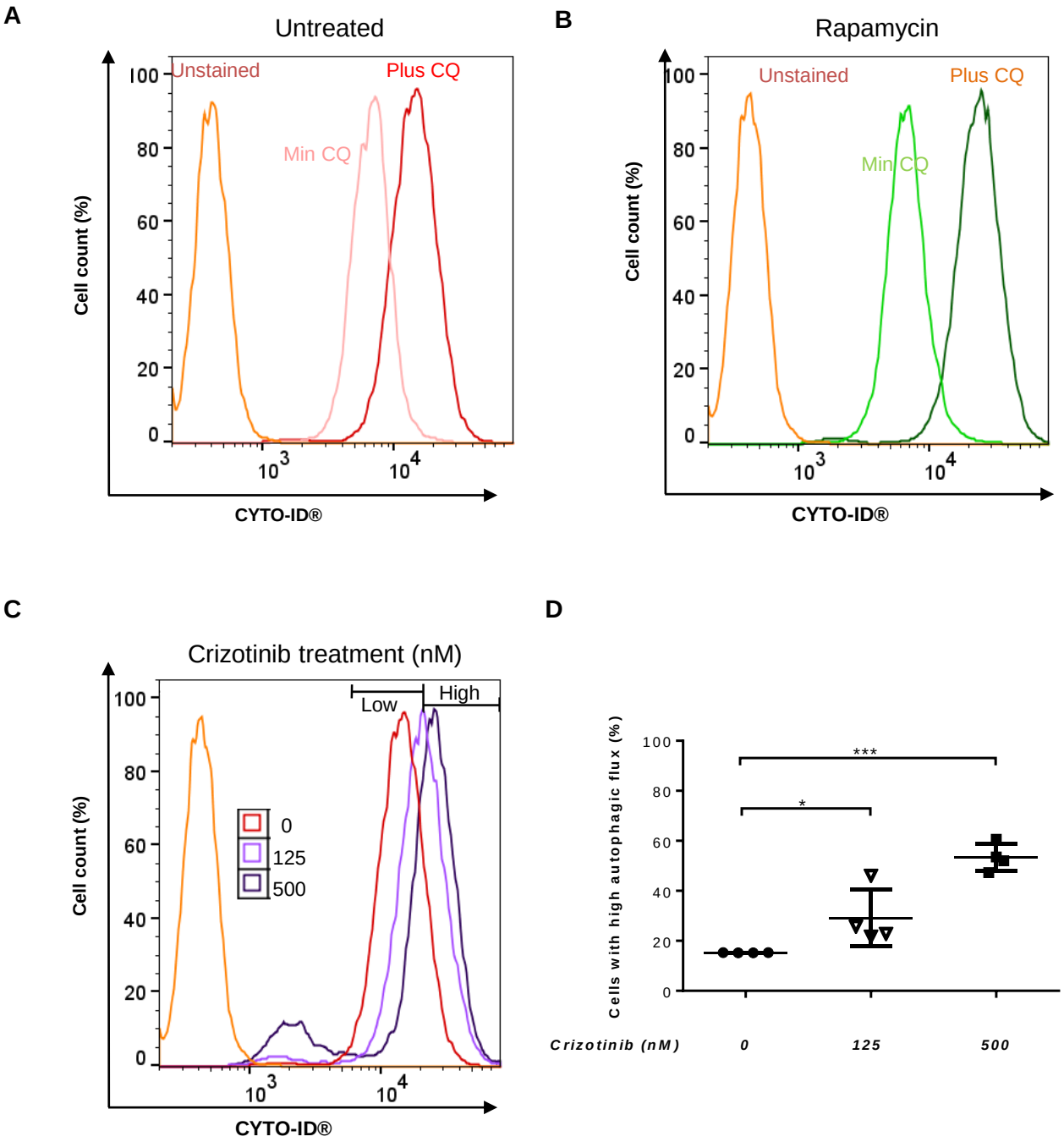

FIGURE S7 : Induction of autophagic flux in response to crizotinib treatment.
KARPAS-299 cells were left untreated or cultured in the presence of rapamycin (positive control) or increasing doses of crizotinib. At the end of the treatments, cells were harvested and stained with the Cyto-ID® Green autophagy dye for flow cytometry analysis. (A and B) Representative FACS plots showing mean fluorescent intensity of Cyto-ID, in the absence or presence of 10µM chloroquine (CQ), in untreated cells or rapamycin-treated cells. (C) Relative accumulation of autophagosomes after 48h treatment with increasing doses of crizotinib (0,125 and 500nM), in the presence of CQ. (D) Histogram representation of enhanced autophagic flux in response to crizotinib treatment. Data represent mean ± SEM; n=4; *p≤0.05; ***p≤0.001; unpaired Student's t test.

FIGURE S8

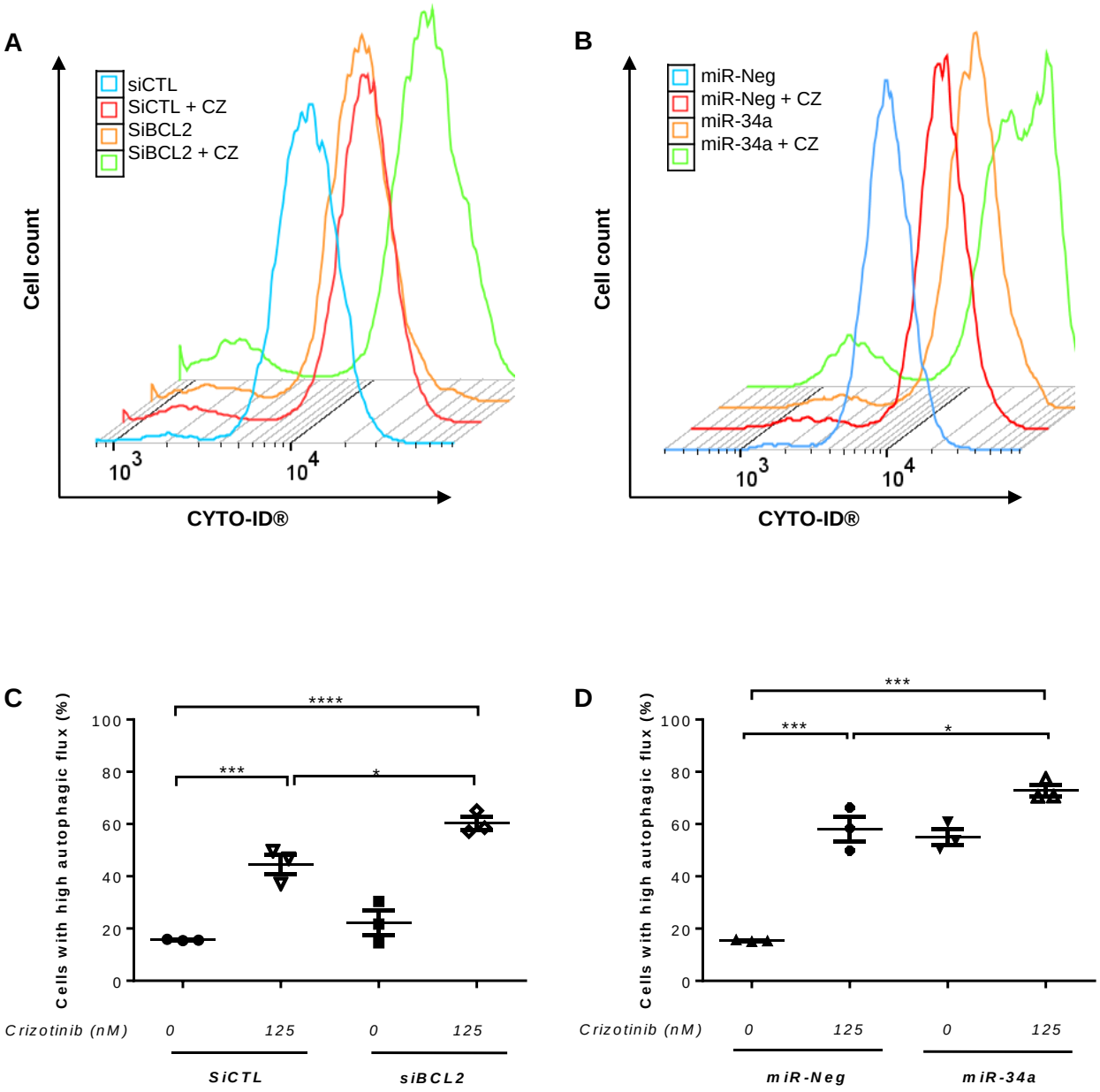

FIGURE S8 : BCL2 downregulation enhances crizotinib-triggered autophagic flux. KARPAS-299 cells were transfected with either siCTL or siBCL2 (A) or miR-Neg and miR-34a mimics (B). 24h later, transfected cells were treated or not with 125 nM crizotinib (CZ) in the presence of chloroquine for a further 48h. (C and D) Histograms representing the percentage of cells with high autophagic flux in response to crizotinib treatment. Data represent mean ± SEM; n=3; *p≤0.05; **p≤0.01; ***p≤0.001; unpaired Student's t test.

FIGURE S9

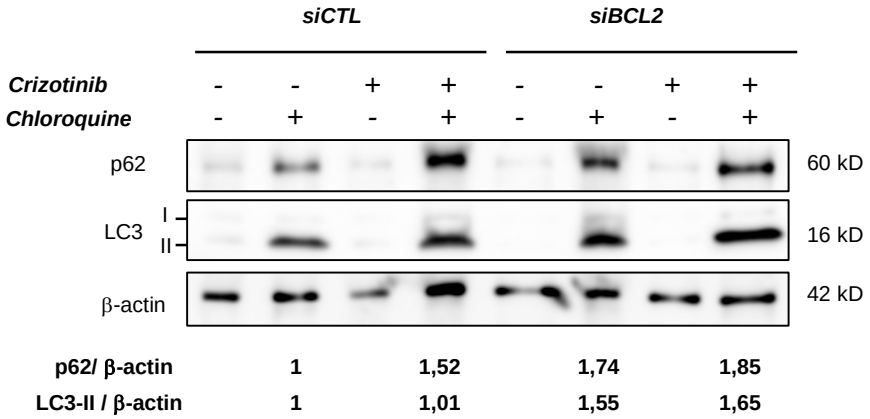

FIGURE S9 : Induction of autophagic flux in response to crizotinib treatment and following BCL2 downregulation. Western blot analysis of p62 and LC3-II accumulation in KARPAS-299 cells that were transfected with either siCTL or siBCL2 in the presence or absence of crizotinib (125nM). 24h after the transfection, KARPAS-299 cells were treated with 125nM crizotinib for a further 48h, in the presence or absence of chloroquine (10µM). Total cell lysates were analyzed by western blotting using antibodies against p62, LC3 and β-actin. β-actin served as the internal control to ensure equal loading. p62/β-actin and LC3-II/β-actin signal ratios were quantified using GelQuantNET; this ratio was set to 1 for the siCTL and chloroquine-treated condition (basal flux).

FIGURE S10

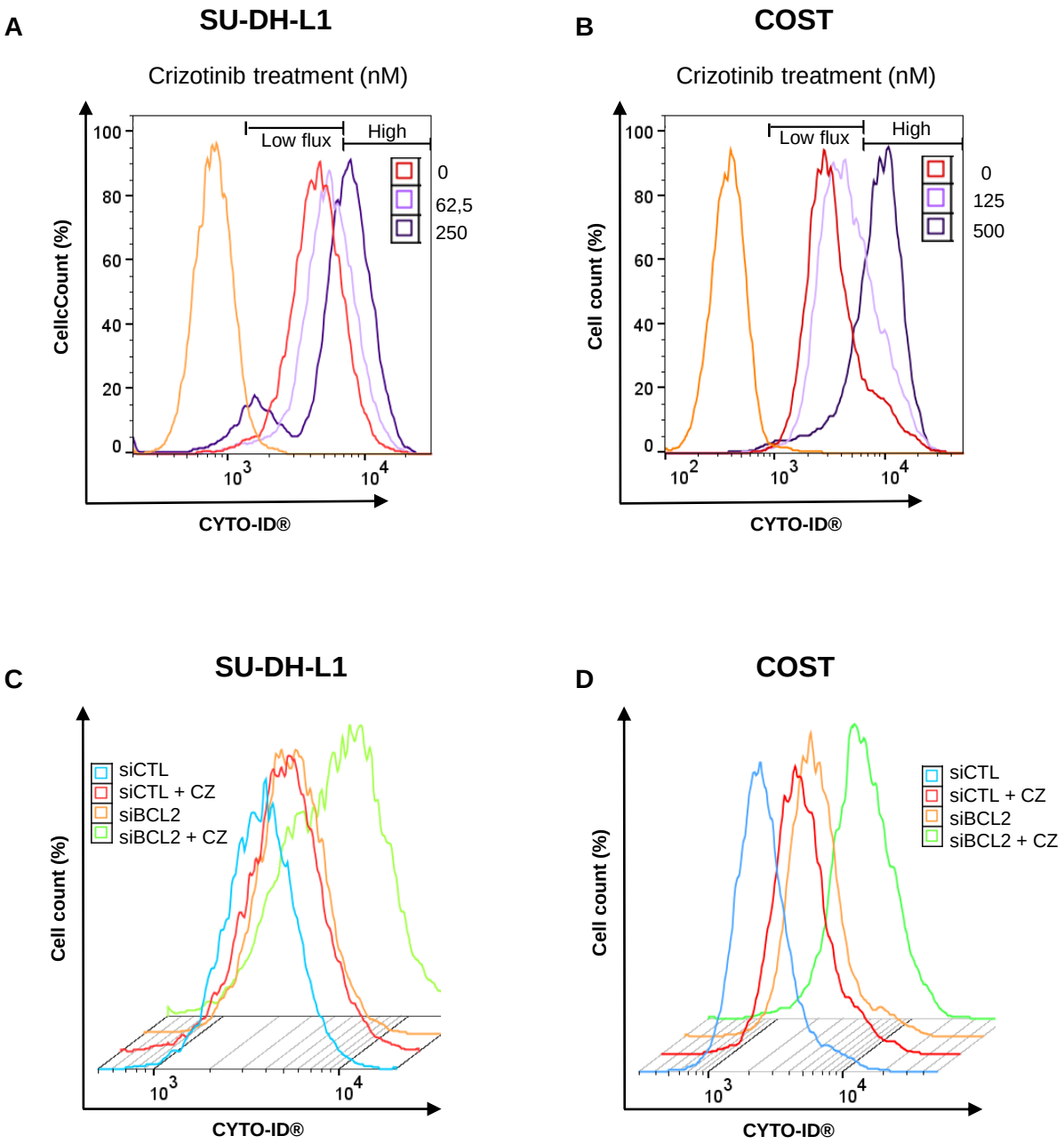

FIGURE S10 : Induction of autophagic flux in response to crizotinib treatment and following BCL2 downregulation in two distinct ALK-positive ALCL cell lines. (A and B) Representative FACS plots showing mean fluorescent intensity of Cyto-ID after treatment with indicated doses of crizotinib (CZ) in the presence of chloroquine (10µM). SU-DHL-1 (A) or COST (B) cells were left untreated or cultured in the presence of increasing doses of crizotinib for 48h. At the end of the treatments, cells were harvested and stained with the Cyto-ID® Green autophagy dye for flow cytometry analysis. (C and D) Flow cytometry analysis of autophagic flux following the knockdown of BCL2 using siCTL or siBCL2 in SU-DHL-1 (C) or COST (D) cells. Cells were transfected with either siCTL or siBCL2. 24h later, they were treated or not with 62,5 nM (SU-DHL-1) or 125 nM (COST) crizotinib in the presence of chloroquine for a further 48h.

FIGURE S11

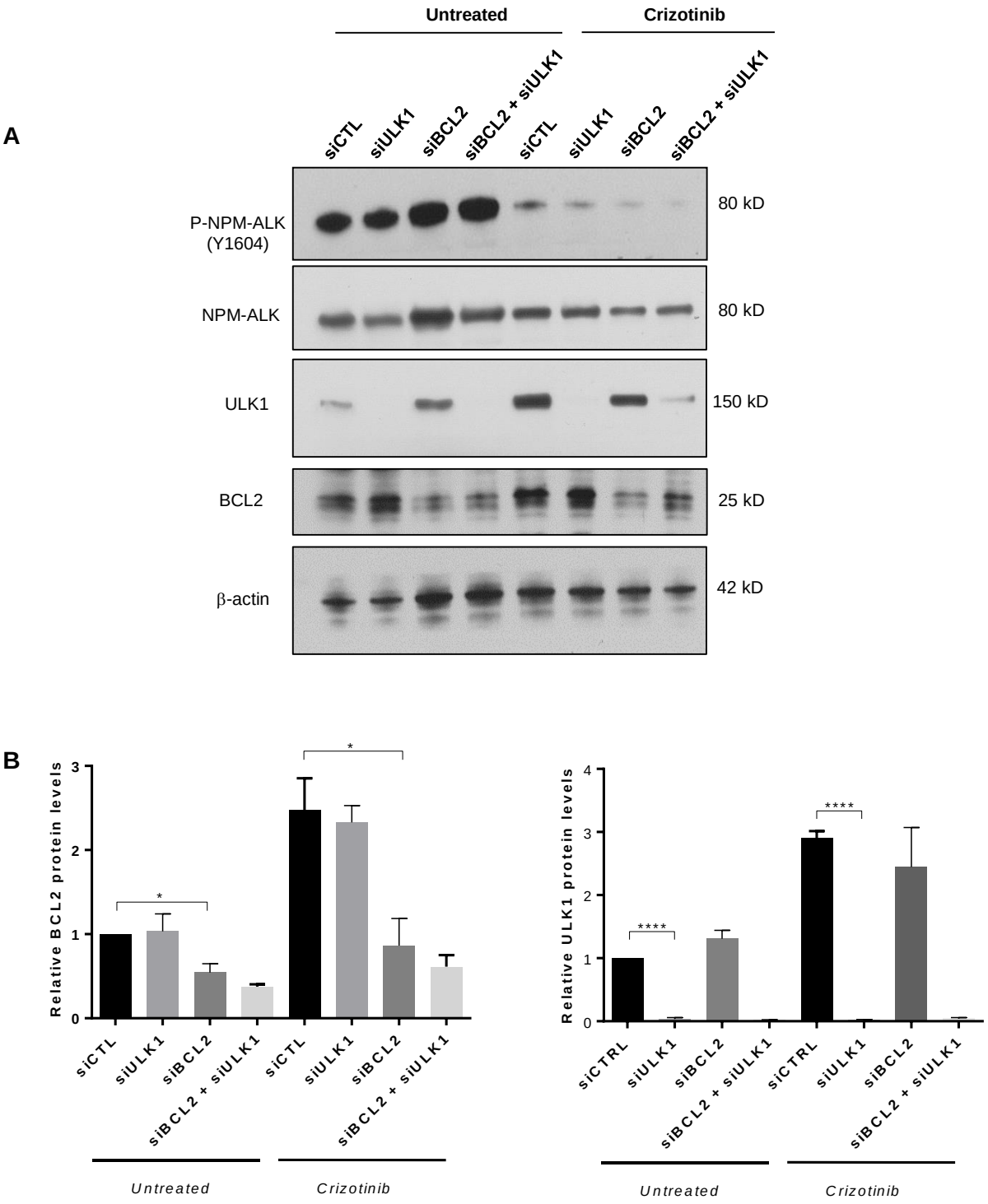

FIGURE S11. BCL2 and ULK1 protein levels following crizotinib treatment of ALK-positive cells that were transfected by targeted siRNAs. (A) Representative Western blot analysis of ULK1 and BCL2 protein levels. Twenty-four hours after transfection with either negative control siCTL, siULK1, siBCL2 or both, mRFP-EGFP-LC3 KARPAS-299 cells were treated (or not) with crizotinib (250nM) for a further 72h. Equal quantities of siRNA were delivered in each condition. β-actin served as the internal control to ensure equal loading. (B) Histogram representations of BCL2 and ULK1 proteins. BCL2/β-actin and ULK1/β-actin signal ratios were quantified using GelQuantNET; these ratios were set to 1 for untreated conditions. Data represent mean ± SEM. n=3, *p≤0.05; ****p≤0.0001; unpaired Student's t test.

FIGURE S12

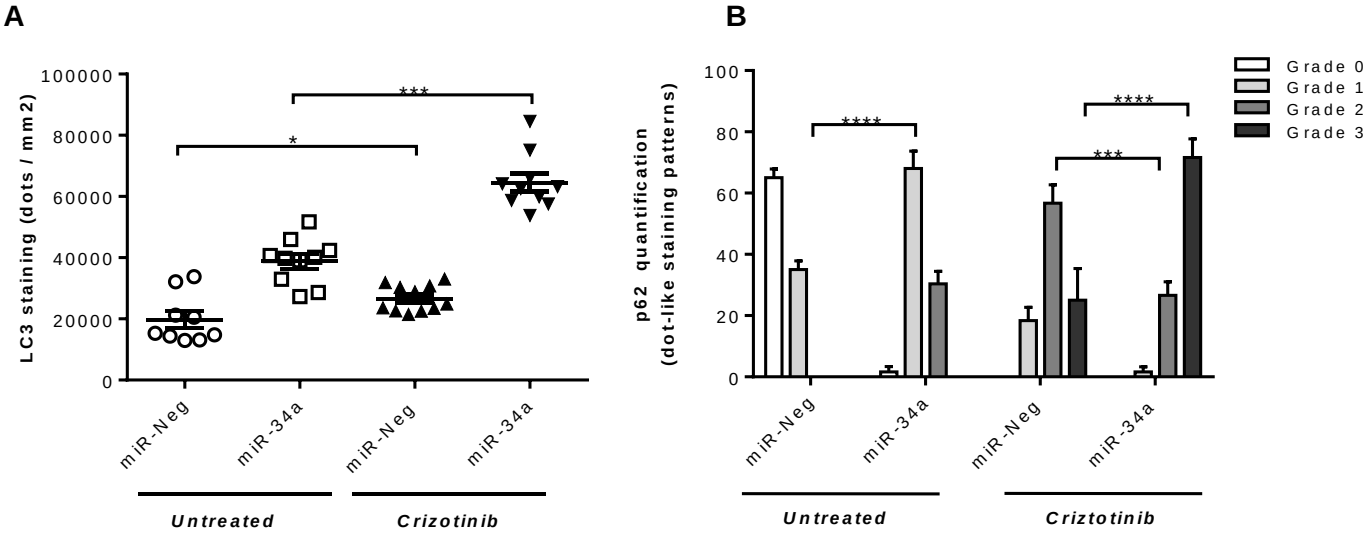

FIGURE S12 : Quantification of two autophagy markers, LC3 and p62, in tumor xenografts. (A) Histogram representation of the number of LC3B positive dots from IHC staining as depicted in Figure 6. LC3 positive dots were quantified using the quantification module of the panoramic viewer software (Supplemental Methods); the Student's t-test was used for side by side comparison of two conditions: *p≤0.05; ***p≤0.001. (B) Histogram representation of p62 relative quantification (See supplemental Methods for details). ***p≤0.001; ****p≤0.0001; unpaired Student's t test.